Proton NMR Study of the Interaction of Tin(IV) Protoporphyrin IX Monomers and Dimers with Apomyoglobin†

Ruba S. Deeb and David H. Peyton*
Chemistry Department, Portland State University, Portland, Oregon 97207-0751
Received July 8, 1991; Revised Manuscript Received September 17, 1991

ABSTRACT: Events during the reconstitution of apomyoglobin to form the holoprotein were probed by porphyrin–metal substitution. Thus interactions between tin(IV) protoporphyrin IX (SnPP) and equine apomyoglobin (apoEqMb), and between tin(IV) protoporphyrin IX dimers [$(SnPP)_2$] and apoEqMb, were observed by ^1H NMR and optical absorbance spectroscopic techniques. The chief advantages of using SnPP are that products and intermediates can easily be related to SnPP·EqMb which has been studied [Deeb, R. S., & Peyton, D. H. (1991) *J. Biol. Chem. 266*, 3728–3733] and that at least one step during reconstitution is slowed considerably as compared to heme. Reactions of apoEqMb with SnPP and $(SnPP)_2$ produce different intermediates, although the final product, SnPP·EqMb, is the same for each. An intermediate observed for reaction of SnPP with apoEqMb at pH 10 is in exchange with free SnPP, with the observed rate constant $k_{off} \sim 1\ s^{-1}$. *meso*-Proton resonances were assigned for this intermediate by correlation to SnPP resonances via chemical exchange. The intermediate observed for reaction of $(SnPP)_2$ with apoEqMb at pH 7.5 is heterogeneous. The reaction of either SnPP or $(SnPP)_2$ with apoEqMb at neutral pH produces another species which may be the alternate porphyrin-insertion isomer arising from a 180° rotation about the α,γ-meso axis of the porphyrin. Although optical absorbance spectroscopy of the Soret region shows evidence for each reaction, only in combination with ^1H NMR are the various processes assigned.

Contributions of the heme prosthetic to protein structure and stability are of continuing interest (Dickerson & Geiss, 1983). The effects of various modifications of parts of the heme have been studied to gain insight into the contribution of the vinyls and the propionates to the equilibrium ratio and reorientation kinetics of the heme-insertion isomers depicted in Figure 1A,B (La Mar et al., 1989, 1991; Hauksson, 1990), but there has been relatively little done to illuminate the role of the porphyrin metal ion. Efforts to observe the alternative isomer failed in freshly-reconstituted protoporphyrin IX·Mb (PPIX-Mb),[1] presumably because the complex rapidly attains the equilibrium state, for which there is only one observable porphyrin-insertion isomer (La Mar et al., 1989; Lecomte & Cocco, 1990).

We therefore decided to study the insertion of metal-*substituted* porphyrins into hemoproteins, with the goal of finding intermediates sufficiently long-lived to allow direct detection by ^1H NMR. Metal substitution may be a lesser perturbation than metal deletion. Tin(IV) protoporphyrin IX (SnPP) is available and interesting in its interactions with heme proteins because of its therapeutic action against hyperbilirubinemia (Muller-Eberhard, 1988; Drummond & Kappas 1982; Drummond & Kappas, 1981). We have reported that the complex SnPP·EqMb has an equilibrium structure strongly analogous to metEqMbH_2O (Deeb & Peyton, 1991). Here we demonstrate by ^1H NMR a relatively long-lived intermediate within the reconstitution process: SnPP + apoEqMb → SnPP-EqMb. Further, the well-characterized monomer–dimer equilibrium of SnPP (Breslow et al., 1986) permits us to directly observe dimeric $(SnPP)_2$ interacting with apoMb but not with the reconstituted protein SnPP·Mb; this interaction was inferred by Breslow et al. (1986) from kinetics arguments alone.

Experimental Procedures

EqMb was from Sigma; apoEqMb was then generated (Teale, 1959). SnPP was from porphyrin products. SnPP solutions were always prepared fresh by dissolving the porphyrin in a minimum amount of base (NaO^2H) in ^1H_2O or ^2H_2O solvent as required. The amount of SnPP added to apoEqMb was determined optically. Titrations and kinetics were performed by measuring optical differences at 418 nm. The optical experiments reported in Figures 5 and 7 were performed in a 5-fold excess of apoEqMb over Sn and were performed generally as in Gebe et al. (1989). All samples containing SnPP were protected from light, and the stability of the samples to light exposure during optical work was verified by obtaining multiple scans on the same sample, whose visible spectrum did not change (Breslow et al., 1986). It should be noted that several of the studies reported here involve nonequilibrium mixtures. Data acquisitions were kept as short as possible in both optical and NMR measurements so as to minimize effects due to averaging. This problem is especially severe for the data reported in Figures 6 and 7, which are for the fastest reaction. Here, each NMR spectrum is unavoidably averaged over a time period of ~0.8 min; in Figure 7 the optical spectra took 3 min for each acquisition, but the time between each wavelength is simply the difference between the start of any two acquisitions.

Infrared spectra were obtained using a Nicolet DX-20 spectrometer with silver chloride sample holders. The solvent

† We thank the Medical Research Foundation of Oregon for a grant. Portland State University, the National Science Foundation, and the Murdock Charitable Trust are recognized for the purchase of the NMR spectrometer.
* The author to whom inquiries about the paper should be addressed.

[1] Abbreviations: EqMb, equine myoglobin; FePPIX, iron(III) protoporphyrin IX, hemin; Mb, myoglobin; NMR, nuclear magnetic resonance spectroscopy; NOE, nuclear Overhauser effect; PPIX, protoporphyrin IX; ROESY, rotating-frame nuclear Overhauser effect spectroscopy; SnPP, tin(IV) protoporphyrin IX; $(SnPP)_2$, dimer of tin(IV) protoporphyrin IX; SwMb, sperm whale myoglobin; T_1^{sel}, selective longitudinal (spin–lattice) relaxation time; TPPI, time-proportional phase incrementation.

0006-2960/92/0431-468$03.00/0

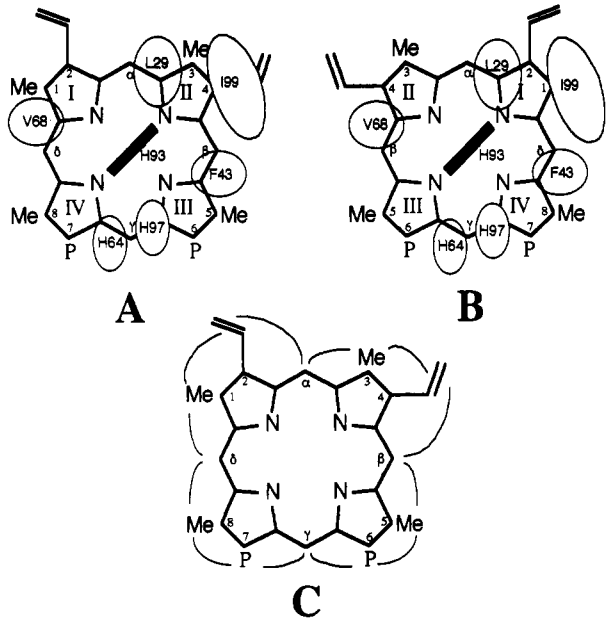

FIGURE 1: Proximal views of the two heme-insertion isomers resulting from a rotation about the α,γ-meso axis in EqMb. (A) Heme-insertion isomer which predominates and is detected in the X-ray crystal structure of EqMb (Evans & Brayer, 1988). (B) Alternate heme-insertion isomer. Residues His[93]F8, His[97]FG3, and Ile[99]FG5 are proximal; the His[93]F8 ring is shown end-on as a bar. Residues Leu[29]B10, Phe[43]CD1, His[64]E7, and Val[68]E11 are distal. (C) PPIX skeleton showing intersubstituent NOEs (arcs) observed in ROESY spectra of SnPP and $(SnPP)_2$.

was either ^2H_2O or 50:50 $^2H_2O/^1H_2{}^{18}O$ to obtain the best window possible in the region between 500 and 1000 cm^{-1} (Caughey, 1980).

The reconstitution of apoEqMb with SnPP was performed in ^2H_2O solvent directly, such that the final concentration was 1–3 mM in 0.5 mL and 200 mM in NaCl. ^1H NMR spectra were recorded on a Bruker AMX-400 NMR spectrometer equipped with a dedicated 5-mm ^1H probe at 25 and 10 °C, operating at 400.14 MHz for ^1H or 149.12 MHz for ^{119}Sn. Spectra were typically collected in quadrature mode with a repetition time of at least 4 s. Chemical shifts were referenced to DSS (2,2-dimethyl-2-silapentane-5-sulfonate) through the residual water signal at 4.76 ppm. 1-D NOE experiments were performed using a preirradiation time of 100 ms in the sequence $(-t_{wt}-t_{irrad}-obs_{90°}-FID-)_n$; saturation-transfer by chemical exchange had irradiation times up to 4 s. At least 64 scans were accumulated for each irradiation frequency, cycling through the decoupling list after each 8 or 16 scans, and 0.3–4 Hz line-broadening factors were applied before Fourier transformation. T_1^{sel} values were estimated by the null method (Harris, 1986). Two-dimensional ROESY (Bax & Davis, 1985; Bothner-By et al., 1984) experiments were performed in the phase-sensitive mode using TPPI (Marion & Wüthrich, 1983).

RESULTS

SnPP and $(SnPP)_2$ ^1H NMR Resonance Assignments. A two-dimensional ROESY spectrum was recorded for SnPP in ^2H_2O at 25 °C, pH 11.5. From this spectrum, we were able to obtain assignments for all SnPP resonances, with the NOEs between the *meso*-H_i and both the $1CH_3$ and $8CH_3$ as the starting point. Intersubstituent NOEs observed are indicated in Figure 1C. A two-dimensional ROESY spectrum was also recorded for $(SnPP)_2$ in ^2H_2O at 25 °C, pH 7.4. Assignments were obtained from a similar protocol. Resonance assignments for SnPP and $(SnPP)_2$ are summarized in Table I. Several of the $(SnPP)_2$ ^1H NMR resonances are split. The most likely explanation for this splitting is that different porphyrin structures are formed (i.e., face-to-face and back-to-back), which are not in fast exchange. Additional splitting of the propionate proton resonances can arise due to inequivalence of geminal protons from restricted rotation within the propionates. Each *meso*-proton resonance is ring-current-shifted upfield by 1.04 ± 0.02 ppm in $(SnPP)_2$ relative to SnPP. This is indicative of a cofacial structure (Johnson & Bovey, 1958), rather than the more usual case of porphyrin aggregation in which there is substantial offset of the two porphyrin rings (Hunter & Sanders, 1990; Abraham & Smith, 1983). The upfield shift of each *meso*-proton from SnPP upon dimerization is almost identical to the ring-current-induced shift of the μ-oxo oligomer $[Sc(octaethylporphyrin)]_2O$ relative to monomeric Sc(octaethylporphyrin)acetate (La Mar et al., 1973). The possibility of a Sn–Sn bond may be eliminated because a much larger upfield shift in the meso resonances would have resulted (Scheer & Katz, 1975).[2] We therefore attempted to observe changes in the infrared spectrum on going from SnPP to $(SnPP)_2$, which would be indicative of the μ-oxo species. There is a weak band at ~988 cm^{-1} in $(SnPP)_2$ which may be due to the Sn–O–Sn asymmetric stretch (Buchler et al., 1973); this band appears to be relocated to ~936 cm^{-1} when the sample is prepared in ^{18}O-enriched water (not shown). This is the isotope effect expected for a μ-oxo metal–O–metal asymmetric stretch (Brown et al., 1969).

Table I: ^1H NMR Chemical Shifts for SnPP Species at 25 °C[a]

assignment	SnPP δ (ppm)	$(SnPP)_2$ δ (ppm)	SnPP·EqMb δ (ppm)	SnPP·EqMb* δ (ppm)
α-meso	10.88	9.86	10.70 (−0.09)[e]	10.65
β-meso	10.83	9.80	10.07 (−0.03)	9.82
γ-meso	10.79	9.73	11.28 (−0.09)	11.14
δ-meso	10.83	9.78[c]	10.64 (−0.02)	10.65
$1CH_3$	3.94	3.94[c]	3.95 (+0.03)	
$3CH_3$	3.90	3.91[c]	4.04 (−0.05)	
$5CH_3$	3.82[b]	3.79[b,c]	2.81 (+0.03)	
$8CH_3$	3.85[b]	3.83[b,c]	3.87 (+0.01)	
$2H_\alpha$	8.59	8.58	8.65 (−0.09)	
$2H_{\beta c}$	6.42	6.66	6.16 (+0.05)	
$2H_{\beta t}$	6.66	6.80	6.10 (+0.02)	
$4H_\alpha$	8.59	8.58	8.78 (−0.04)	8.61
$4H_{\beta c}$	6.42	6.66	6.81 (+0.07)	
$4H_{\beta t}$	6.66	6.80	6.94 (+0.04)	
$6,7H_{\alpha,\alpha'}$	4.59	4.63, 4.52[d]		
$6,7H_{\beta,\beta'}$	3.25	3.16, 3.05[d]		

[a] SnPP at pH 11.5; $(SnPP)_2$ at pH 7.5; SnPP·EqMb at pH 10.1; SnPP·EqMb* at pH 10.2. [b] The $5CH_3$ and $8CH_3$ assignments may be reversed for SnPP and $(SnPP)_2$. [c] These peaks are split into two peaks in the dimer; chemical shifts are averages. [d] These peaks are very complex multiplets in the dimer; chemical shifts are averages. [e] Numbers in parentheses indicate chemical shift changes on titrating from pH 10.1 to 7.0. Negative numbers indicate upfield shifts.

^1H NMR Observation of an Intermediate in the Process: SnPP + apoEqMb → SnPP·EqMb. The downfield region at 25 °C and pH 10.2 is shown in Figure 2A,D for apoEqMb, after ~5 and ~400 min after mixing with an excess of SnPP. SnPP·EqMb (Deeb & Peyton, 1991) is the final product,

[2] ^{119}Sn NMR also provides evidence that there is no Sn–Sn bond; such a structure for $(SnPP)_2$ would have a coupling constant between ^{117}Sn and ^{119}Sn (each nucleus is present at ~8%); such one-bond couplings are on the order of 1–4.5 kHz (Harris et al., 1978). No such coupling was visible. Small peaks at the putatively much smaller Sn–O–Sn coupling, ~300 Hz, are observed, although the presence of multiple $(SnPP)_2$ species leads to broadening of all the peaks, and so the identity of peaks as arising from J coupling (each at ~4% of the major peak) is not certain. The ^{119}Sn chemical shift change on going from SnPP to $(SnPP)_2$ is only +13.1 ppm; this suggests that Sn-coordination number remains the same (six) for these two species (Harris et al., 1978).

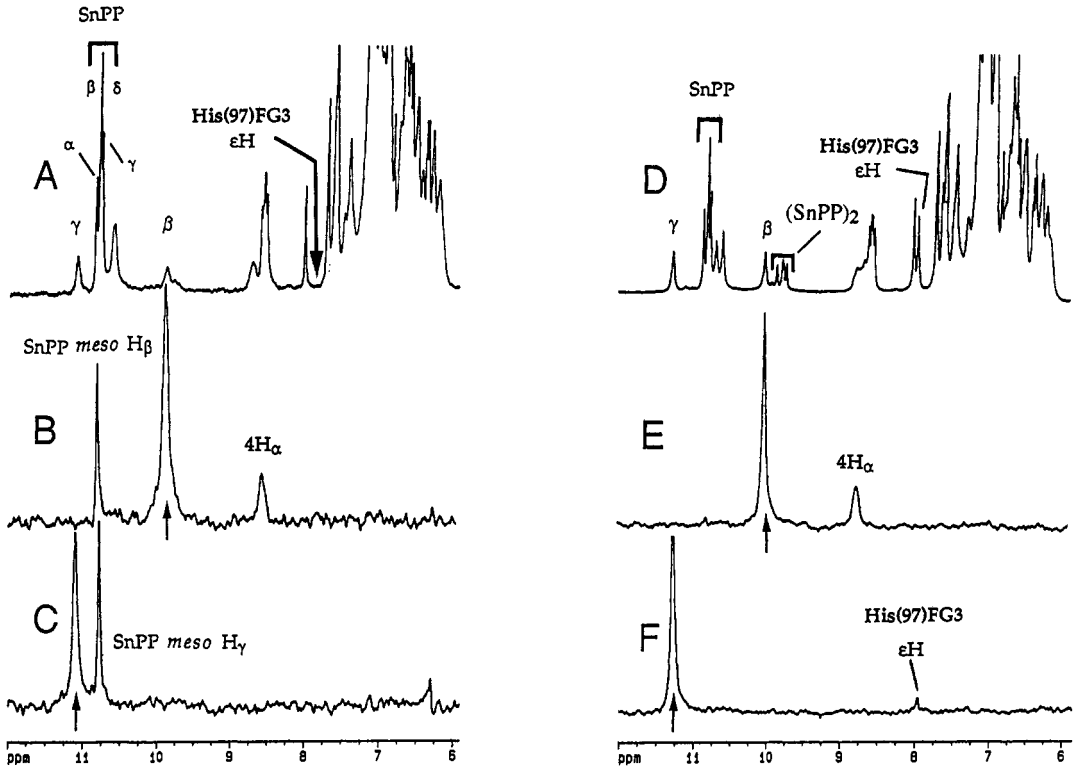

FIGURE 2: Saturation-transfer for SnPP·EqMb* and SnPP·EqMb in the presence of excess SnPP monomer at pH 10.2 and 25 °C. (A) Reference spectrum recorded immediately after reconstitution; note the missing εH from $His^{97}FG3$. (B) Difference spectrum resulting from irradiating at the position labeled β in reference trace A. Note both NOE to the heme vinyl H_α at 8.6 ppm and magnetization transfer to the free monomer *meso*-H_β. (C) Difference spectrum resulting from irradiating at the position labeled γ in reference trace A. Note the magnetization transfer to the free monomer *meso*-H_γ. (D) Reference spectrum recorded after the sample from trace A has nearly attained equilbrium (400 min after reconstitution). Note that the εH from $His^{97}FG3$ is present. A small amount of $(SnPP)_2$ is evident in this spectrum. (E) NOE difference spectrum resulting from irradiating the *meso*-H_β of SnPP·EqMb. (F) NOE difference spectrum resulting from irradiating the *meso*-H_γ of SnPP·EqMb. Note that the expected NOEs to vinyl $4H_\alpha$ from *meso*-H_β and to εH of $His^{97}FG3$ from *meso*-H_γ are present but that there is no saturation-transfer to free SnPP *meso*-H's.

shown in Figure 2D. At early times after mixing (Figure 2A), an intermediate is evident from the *meso*-proton shifts, in that they are different from those of SnPP·EqMb; a resonance from His FG3 is also shifted in SnPP·EqMb*. Hereafter we denote the intermediate detected in Figure 2A as SnPP·EqMb*. Saturation transfer via chemical exchange between *meso*-protons from SnPP and SnPP·EqMb* is shown in Figure 2B,C (note that the excess SnPP provides the opportunity to observe chemical exchange between SnPP·EqMb* *meso*-H's and the free SnPP, and hence the assignments for SnPP·EqMb* *meso*-H's). Analogous saturation transfer by chemical exchange between SnPP and the final species SnPP·EqMb is not observed (Figure 2E,F). In Figure 3 are results of a reconstitution of SnPP into apoEqMb at 10 and 25 °C. At the lower temperature, chemical exchange would be attenuated, while any NOEs would become more negative owing to the increased correlation time of the protein. In fact, the magnetization transfer from the *meso*-H_β proton in SnPP·EqMb* is diminished at lower temperature (compare Figure 3 panel B to panel C). The assignments for SnPP in solution (above) combined with the saturation-transfer by chemical exchange in Figures 2 and 3 permit us to make the *meso*-proton assignments for SnPP·EqMb* as indicated in Figure 2 and Table I.[3]

SnPP·EqMb* has its upfield resonance from $Val^{68}E11$ γCH_3 at almost the same chemical shift as does SnPP·EqMb; Figure 4A is a reference spectrum recorded at intermediate time to show both species. Figure 4B shows the NOE difference spectrum resulting from irradiating at the position of the $Val^{68}E11$ γCH_3 resonance from SnPP·EqMb*. Figure 4C shows the NOE difference spectrum resulting from irradiating at the position of the $Val^{68}E11$ γCH_3 resonance of the equilibrium species SnPP·EqMb. Both NOE difference spectra show NOEs to the position of the heme *meso*-H_δ (although in SnPP·EqMb* the *meso*-H_δ and -H_α overlap), as well as to the indicated $Val^{68}E11$ resonances; the position of the $Val^{68}E11$ αH in Figure 4B is somewhat downfield of its equilibrium location at 2.74 ppm (Figure 4C; Deeb & Peyton, 1991). There are also NOEs observed to $Leu^{29}B10$ analogous to the equilibrium species. We conclude that SnPP·EqMb* has the distal side of the porphyrin-binding pocket very similar to that of SnPP·EqMb, including predominantly a single porphyrin-insertion isomer.

Optical Spectroscopic Observation of an Intermediate in the Process: SnPP + apoEqMb → SnPP·EqMb. The spectra in Figure 5A demonstrate the time dependence for the Soret region from the reconstitution of SnPP into apoEqMb; Figure 5B shows difference spectra for this reaction. This result is reminiscent of the optical spectra obtained for the reconstitution of heme into apoSwMb (Gebe et al., 1989). In that case, however, the initially observed species was a 1:1 mixture of heme-insertion isomers (Jue et al., 1983), while here the initially observed species is not a mixture, at least as we can detect by ^1H NMR. The isosbestic point in the optical spectra reflects a conversion of one species to another species—explicitly, SnPP·EqMb* to SnPP·EqMb. The shift in λ_{max} is from ~416 nm (SnPP·EqMb*) to ~417 nm (SnPP·EqMb);

[3] The assignment of *meso*-H_γ in SnPP·EqMb* is straightforwardly related to the SnPP *meso*-H_γ by saturation transfer, but overlap between SnPP *meso*-H_β and *meso*-H_δ resonances introduces an ambiguity into the assignment of *meso*-H_β in SnPP·EqMb*. This is, however, resolved by the NOE in Figure 2B to a porphyrin vinyl-H_α, which dictates the irradiated resonance as arising from the SnPP·EqMb* *meso*-H_β.

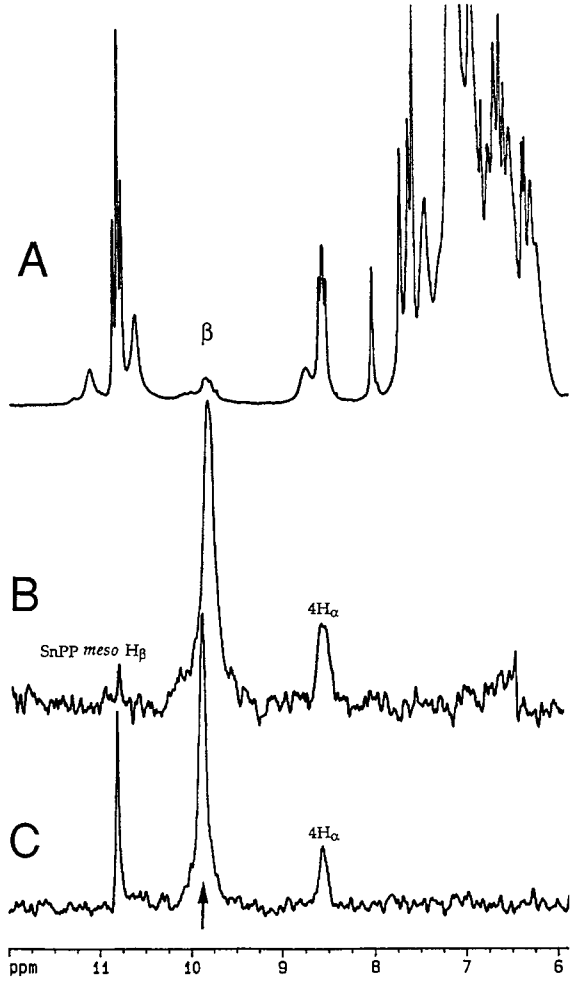

FIGURE 3: Saturation-transfer difference spectra for SnPP·EqMb* in the presence of excess SnPP monomer at pH 10.2, at 10 and 25 °C. (A) Reference spectrum recorded immediately after reconstitution. (B) Difference spectrum resulting from irradiating at *meso*-H_β of SnPP·EqMb* at 10 °C. (C) Difference spectrum resulting from irradiating at *meso*-H_β of SnPP·EqMb* at 25 °C. Note the diminished saturation-transfer at the lower temperature (trace B) and the increased NOE to heme vinyl $4H_\alpha$.

for the free porphyrin, λ_{max} is ~407 nm (SnPP, pH 10.2) and the band shape is similar to those shown in Figure 5A (Breslow et al., 1986).

^1H NMR Observation of an Intermediate in the Process: $(SnPP)_2$ + 2apoEqMb → 2SnPP·EqMb. Figure 6 presents the *meso*-proton region for the reaction between $(SnPP)_2$ and apoEqMb at pH 7.5. Figure 6A shows the meso region of a ^1H NMR spectrum of $(SnPP)_2$. Figure 6B was acquired 2–2.8 min after combining $(SnPP)_2$ with apoMb. The *meso*-proton peaks from $(SnPP)_2$, now marked by asterisks (*), are poorly resolved and generally shifted upfield relative to $(SnPP)_2$. Clearly, the porphyrin is interacting with apoEqMb but still is a dimer as indicated by the *meso*-proton chemical shifts which reflect the ring-current shift from the alternate porphyrin ring. Further evidence, from visible spectroscopy, that SnPP remains a dimer in $(SnPP)_2$·EqMb is presented below. Figure 6C was acquired 10–13 min after combining $(SnPP)_2$ with apoEqMb. A significant amount of SnPP·EqMb is now observed; the remaining $(SnPP)_2$·EqMb signals have a different overall appearance in Figure 6C than in Figure 6B. $(SnPP)_2$·EqMb is therefore heterogeneous. Figure 6, acquired 118–121 min after combining $(SnPP)_2$ with apoMb, shows only the equilibrium species SnPP-EqMb. A second aliquot of $(SnPP)_2$ added to the product of Figure 6D produces the spectrum of 6E, which can be described as an approximate linear combination of Figure 6 panels A and D: $(SnPP)_2$ appears not to interact with SnPP·Mb.

Another species in Figure 6C is indicated with arrows; we designate this new species as SnPP·EqMb′. SnPP·EqMb′ cannot be SnPP·EqMb* because its characteristic *meso*-H_γ resonance is missing from ~11.1 ppm,[4] nor can it originate from $(SnPP)_2$ or $(SnPP)_2$·EqMb because reconstitution of excess apoEqMb at neutral pH with a small aliquot of SnPP produces SnPP·EqMb′ without detectable formation of $(SnPP)_2$ or $(SnPP)_2$·EqMb (the rate of dimerization is much slower than insertion into apoEqMb). SnPP·EqMb′ unfortunately is never present in sufficient quantity to allow us to observe NOEs from its *meso*-H resonances. The identity of SnPP·EqMb′ is discussed below.

Optical Spectroscopic Observation of the Kinetics of the Process: $(SnPP)_2$ + 2apoEqMb → 2SnPP·EqMb. The spectra in Figure 7A demonstrate the time course for the Soret region from the reconstitution of $(SnPP)_2$ into apoEqMb; Figure 7B shows difference spectra for this reaction. ApoMb was in excess, so that the initial species is $(SnPP)_2$·EqMb, as seen in the NMR spectrum of Figure 6B; the band is broadened, lowered in intensity, and at shorter wavelength, ~387 nm. These are characteristic of the porphyrin being a dimer [λ_{max} ~ 386 nm [$(SnPP)_2$]; λ_{max} ~ 407 nm (SnPP)]. The final species in Figure 7A is characteristic of SnPP·EqMb (λ_{max} ~ 416 nm, pH 7.1). Although the NMR spectra shown in Figure 6B,C dictate that $(SnPP)_2$·EqMb must be heterogeneous and its components change in ratio with time, the optical spectra are quite insensitive to this. Conversion to SnPP·EqMb must occur with loss of dimer, and, in agreement with Breslow et al. (1986), we find that the rate of dimer dissociation is enhanced in the presence of apoEqMb (by a factor of ~2).

Discussion

Evidences from ^1H NMR, ^{119}Sn NMR, and infrared spectroscopy about the structure of $(SnPP)_2$ are consistent with a μ-oxygen bridged oligomer. The alternative dimer, formed by π–π interactions (Hunter & Sanders, 1990), would be expected to produce an offset geometry for the highly unsymmetric porphyrin core of SnPP, and this would have produced greatly different shifts among the *meso*-protons upon dimerization (e.g., Abraham et al., 1976; Abraham & Smith, 1983). The evidence from ^{119}Sn NMR indicates that $(SnPP)_2$ has two axial ligands;[2] it seems unlikely that the cofacial geometry would be possible without oxygen bridging. The very slow exchange between SnPP and $(SnPP)_2$ (Breslow et al., 1986) would also be unusual for π–π interaction (Scheer & Katz, 1975; Pasternack et al., 1973). Nevertheless we regard the conclusion that $(SnPP)_2$ is a μ-oxygen bridged oligomer as tentative until $(SnPP)_2$ and/or related porphyrins are isolated and characterized more fully. Even if $(SnPP)_2$ has an oxygen bridge, it may be protonated as has been postulated for an Fe^{III}(tetracarboxyphenylporphyrin) in water solvent (Stong & Hartzell, 1976). We are currently pursuing studies of other Sn-porphyrins, which should lead to a more definitive characterization of the dimer species.

We can infer structural information about SnPP·EqMb* from the following observations. First, the chemical shift and NOEs from upfield $Val^{68}E11$ γCH_3 are virtually identical for SnPP·EqMb and SnPP·EqMb* (Figure 4): the distal side of

[4] A pH-jump experiment demonstrated that SnPP·EqMb* is converted to SnPP·EqMb within <1 min at neutral pH with no detectable SnPP·EqMb′ formed. Therefore, SnPP·EqMb′ and SnPP·EqMb* are different species.

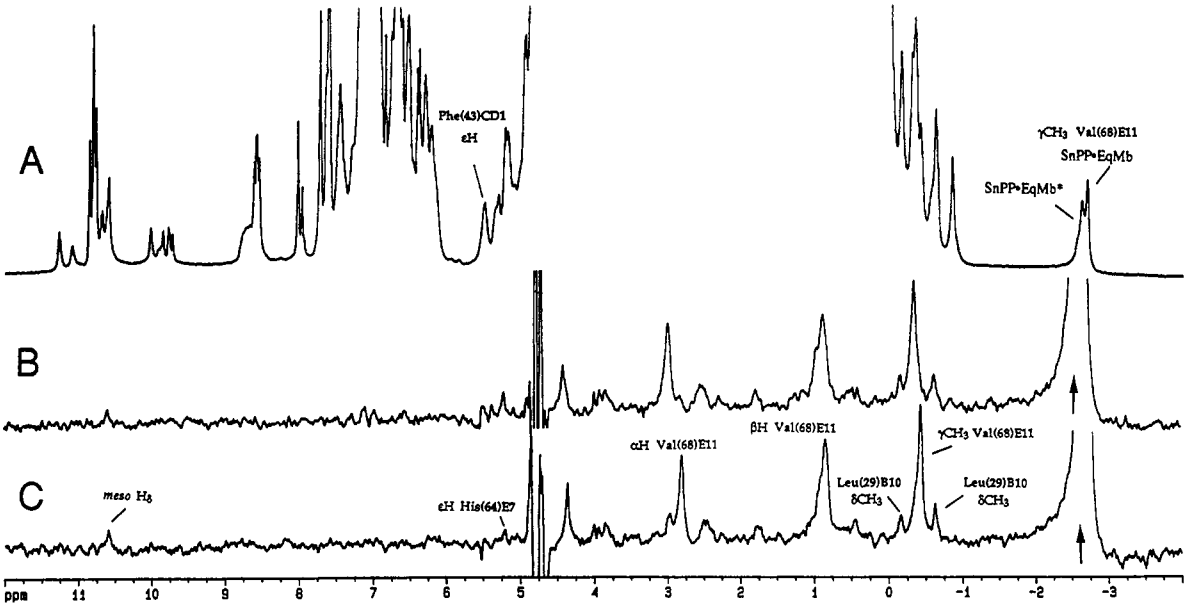

FIGURE 4: NOE difference spectra resulting from irradiating the upfield resolved Val[68]E11 γCH_3 at pH 10.2 and 25 °C. (A) Reference spectrum recorded at intermediate time, showing both SnPP•EqMb and SnPP•EqMb*. (B) NOE difference spectrum resulting from irradiating Val[68]E11 γCH_3 from SnPP•EqMb*. (C) NOE difference spectrum resulting from irradiating Val[68]E11 γCH_3 from SnPP•EqMb. Note the correspondence of the NOE difference traces, including to the heme *meso*-H_δ, indicating that the distal residues Val[68]E11, Leu[29]B10, and probably His[64]E7 are in approximately the same orientations relative to each other and to the heme. Note also the εH from Phe[43]CD1, which is at the same chemical shift in both species.

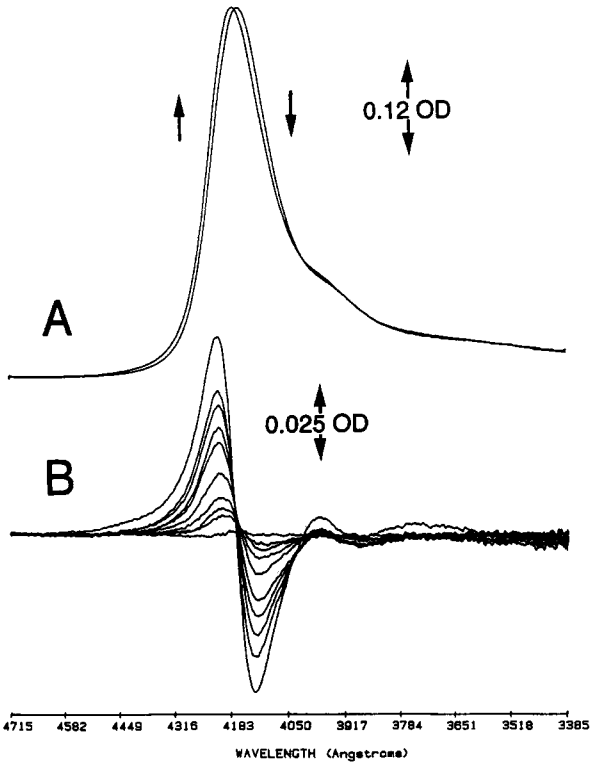

FIGURE 5: Optical spectra of the Soret region which reflect the conversion of SnPP•EqMb* to SnPP•EqMb at pH 10.0 and 25 °C. (A) Spectra recorded at ~1 (right) and 132 (left) min after reconstitution. Note that the right spectrum corresponds to the species reported in Figure 2A, while the left spectrum corresponds to SnPP•EqMb, the species reported in Figure 2D. (B) Difference spectra resulting from subtracting spectra recorded at various times (1, 6, 10, 14, 18, 23, 37, 46, 61, and 103 min) from the final spectrum (132 min). The rate constant for this process is calculated: $k \sim 4 \times 10^{-2}$ min^{-1}.

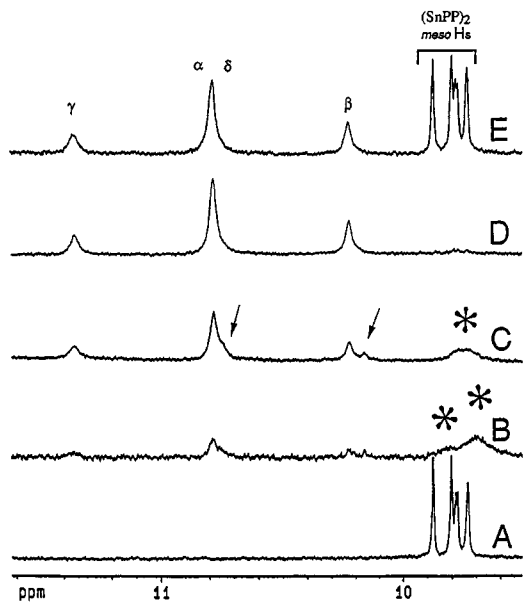

FIGURE 6: ^1H NMR observation of the incorporation of $(SnPP)_2$ into apoEqMb in the downfield region at pH 7.5 and 25 °C. (A) Spectrum of $(SnPP)_2$. (B–D) Spectra recorded at ~2.5, 12, and 120 min after mixing $(SnPP)_2$ with apoEqMb. (E) Spectrum recorded after adding a second equivalent of $(SnPP)_2$ to the sample from spectrum D. Note that $(SnPP)_2$ appears not to interact with SnPP•EqMb (E) but interacts with apoEqMb (B–D).

the porphyrin-binding pocket is largely intact in the vicinity of this residue. Second, the off-rate for SnPP from SnPP•EqMb* is estimated (from the magnitude of saturation transfer and T_1^{sel} of free SnPP *meso*-protons, ~0.5 s) to be ~1 s^{-1} (Sandström, 1982): the proximal His[64]E7-Sn bond is almost certainly missing. Third, SnPP•EqMb* does not have His[97]FG3 γH at its usual chemical shift (compare Figure 2 panels A and D): the salt bridge between His[97]FG3 and the heme 7-propionate may not be formed or may be in a perturbed conformation. The resulting picture for SnPP•EqMb* has SnPP inserted into the globin in approximately the same way as in SnPP•EqMb or the heme in Mb, but with the proximal His[93]F8 not coordinated to the Sn, and the 7-propionate to His[97]FG3 H-bond either missing or different from its native structure. We have provided evidence that in SnPP•EqMb the Sn–His[93]F8 bond is indeed present (Deeb &

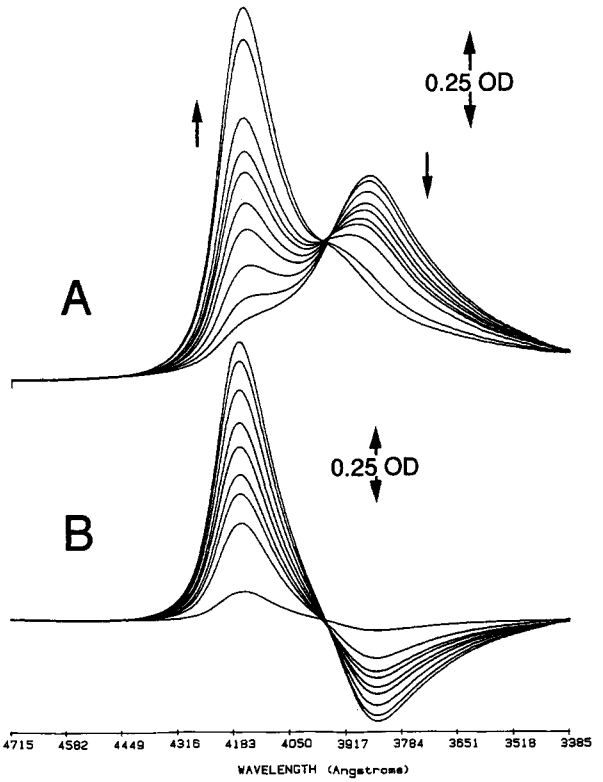

FIGURE 7: Optical spectra of the Soret region which reflect the conversion of $(SnPP)_2$·EqMb to SnPP·EqMb at pH 7.1. (A) Spectra recorded at ~1, 5, 13, 23, 32, 44, 53, 62, 154, and 258 min after reconstitution. Note that the first spectrum corresponds to the species shown in Figure 6B, while the last spectrum corresponds to SnPP·EqMb, the species shown in Figure 6D. Also note that $\lambda_{max} \sim 387$ nm for $(SnPP)_2$·EqMb is virtually identical to that of $(SnPP)_2 \sim 386$ nm (Breslow et al., 1986): the porphyrin is therefore still dimerized. (B) Difference spectra resulting from subtracting spectra recorded at various times (1, 5, 13, 23, 32, 44, 53, 62, and 154 min) from the final spectrum (258 min). The rate constant is calculated: $k \sim 2 \times 10^{-2}$ min^{-1}.

Peyton, 1991), as is the 7-propionate–His^{97}FG3 salt bridge as suggested by the chemical shift of the His^{97}FG3 γH resonance. The distal position appears to be occupied by water, as revealed by *meso*-proton pH-titration behavior (Deeb & Peyton, 1991).

La Mar et al. (1989) and Lecomte and Cocco (1990) tried to observe the formation of porphyrin-insertion isomers in freshly prepared PPIX·SwMb and PPIX·EqMb, respectively. The lack of the proximal His^{93}F8–metal bond was invoked to explain rapid approach to an equilibrium distribution of heme-insertion isomers, so that only a single porphyrin-insertion isomer could be observed in the time required to obtain an NMR spectrum. Our data here support this idea of rapidly exchanging porphyrin-insertion isomers if the His^{93}F8–metal bond is missing. In fact, the estimated rate of SnPP dissociation from SnPP·EqMb*, $k_{off} \sim 1$ s^{-1}, is a lower bound for porphyrin-insertion isomer redistribution for SnPP·EqMb* because porphyrin reorientation is not supposed to require complete dissociation from the globin (La Mar et al., 1984). The notion that the metal–His^{93}F8 bond might be relatively slow to form in some cases is supported by optical studies of the formation of metEqMbCN from hemin dicyanide and apoEqMb (Kawamura-Konishi et al., 1988), for which the step assigned as formation of the Fe–His^{93}F8 bond was rate limiting.

La Mar et al. (1989) found that the position occupied by the 6-propionate in native Mb forms the *initial* H-bond when reconstituting SwMb with either 6-methyl-6-despropionate hemin or 7-methyl-7-despropionate hemin. The residue involved in this salt bridge is Arg^{45}CD3 (Lys in EqMb); this residue's side chain has been found to be disordered in the CO complex of SwMb (Kuriyan et al., 1986), and this disorder may be a part of the mechanism of ligand binding by the globin. We find that ϵH from His^{97}FG3, which forms the salt bridge to the 7-propionate, is absent from its usual resonance position in SnPP·EqMb*; this resonance is observed only when the final species, SnPP·EqMb, is formed. His^{97}FG3 is separated from His^{93}F8 by only three residues, and the F-helix is likely not in the native position in SnPP·EqMb*, as may be the case in apoEqMb (Hughson et al., 1990; Cocco & Lecomte, 1990). We have no assignments for Lys^{45}CD3 in SnPP·EqMb and so have no direct evidence about the state of the salt bridge to the 6-propionate in SnPP·EqMb*. However the adjacent residue, Phe^{46}CD4, is in about the same position as in SnPP·EqMb (the peak for the ϵHs are at approximately the same position throughout; Figure 4), strongly ring-current-shifted by the porphyrin, so it is reasonable that Lys^{45}CD3 is also approximately in its native spatial position, with the salt bridge to the 6-propionate formed.

The insertion of $(SnPP)_2$ into apoMb is perhaps the most surprising part of this work because the X-ray crystal structures for Mb have the native porphyrin (heme) tightly enclosed within the protein, so there seems to be no room for species as wide as a porphyrin dimer (Evans & Brayer, 1988). Both the meso ^{1}H NMR chemical shifts of $(SnPP)_2$ and X-ray structures of μ-oxo metalloporphyrin oligomers (Hoffman et al., 1972) suggest that the width of the dimer is in the ~6 Å (Sn-to-Sn centers separated by ~4 Å). However, apoMb has a reduced helical content relative to the holoprotein (Breslow et al., 1965; Harrison & Blout, 1965), and it may be that the F-helix is partly or largely unfolded [Hughson et al. (1990) and above]. Such a structural perturbation could provide sufficient room and/or flexibility at the nascent heme pocket in apoMb for $(SnPP)_2$ to interact. An analogous structure involving *heme* may be a detectable intermediate by the methods analogous to those of Kawamura-Konishi et al. (1988) if a significant amount of heme were to be dimer, rather than higher aggregates. For the present case, it is fortunate that the monomer–dimer equilibrium of SnPP is slow enough to allows us to monitor such changes directly by NMR methods.

We finally turn to the question of the structure of SnPP·EqMb′, the species indicated by arrows in Figure 6C. SnPP·EqMb′ is not detected when reconstitutions are carried out at high pH. The 10.17 ppm resonance may be from the *meso*-H$_\delta$ of the porphyrin-insertion isomer shown in Figure 1B; the chemical shift interchange of *meso*-protons under an α,γ-meso axis formal rotation in diamagnetic hemoglobins has been reported (Cooke & Wright, 1987; La Mar et al., 1989). Also as in those reports, we see evidence of the two porphyrin-insertion isomers as an additional resonance from upfield Val^{68}E11 γCH$_3$ (not shown) (Jue et al., 1983). The identified SnPP·EqMb′ peaks correspond well to the pattern of the minor heme-insertion isomer peaks of SWMbCO (La Mar et al., 1989; 1983): minor peak Val^{68}E11 γCH$_3$ downfield of the major peak, minor peak γ-meso just upfield of the major β-meso peak, and minor β-meso peak apparently overlapping major γ-meso peak. As noted above, it is unfortunate that SnPP·EqMb′ is present in too low an amount at equilibrium and disappears too rapidly after reconstitution to permit NOE studies. Nevertheless, the observation of SnPP·EqMb′ only at neutral pH is reasonable for the alternate porphyrin-insertion isomer because the ligand water, as opposed to hydroxy, could be replaced by His^{93}F8 quickly enough to trap both

porphyrin-insertion isomers depicted in Figure 1A,B.

Cowan and Gray (1989) suggested that splitting of Q-bands in the 450–650 nm region of the optical spectrum of metal-substituted porphyrin reconstituted SwMb, including SnPP·SwMb, can be attributed to the presence of the porphyrin-insertion isomers shown in Figure 1. Although Cowan and Gray used SwMb, the Q-bands for SnPP·EqMb are nearly identical (not shown). Our previous work (Deeb & Peyton, 1991) showed that there is only one SnPP-insertion isomer in equilibrium SnPP·EqMb, at least as detectable by ^{1}H NMR. In spectra of samples aged at least 12 h, recorded to very high signal-to-noise ratio, no SnPP·EqMb′ is detected: SnPP·EqMb′, the only species we have observed which could be the porphyrin-insertion isomer depicted in Figure 1B, is present at most to a few percent at equilibrium. Therefore the amount of Q-band splitting in SnPP·Mb must be due in major part to factors other than the presence of porphyrin-insertion isomers, although some contribution by porphyrin-insertion isomers cannot be excluded.[5] DiFeo and Addison (1991) reached a similar conclusion for iron porphyrin–globin complexes.

Structural characterization of a species analogous to SnPP·EqMb* in reconstitution reactions involving heme has not been reported. The reason for this is the fast rate for formation of the Fe–His^{93}F8 bond (Kawamura-Konishi et al., 1988). Only a very slow to dissociate ligand, such as cyanide, might afford the opportunity to observe such a species by ^{1}H NMR. We have not been able to detect such a species directly. However, the ratio of heme-insertion isomers from the reaction between apoMb and hemin dicyanide does, in fact reflect a heme-insertion isomer *reorientation* occurring before Fe–His^{93}F8 bond formation (Yee & Peyton, 1991). Therefore SnPP·EqMb* is an interesting and long-lived model for a very short-lived species along the heme-insertion reaction pathway for Mb.

References

Abraham, R. J., & Smith, K. M. (1983) *J. Am. Chem. Soc. 105*, 5734–5741.

Abraham, R. J., Eivazi, F., Pearson, H., & Smith, K. M. (1976) *J. Chem. Soc., Chem. Commun. 1976*, 699–701.

Bax, A., & Davis, D. G. (1985) *J. Magn. Reson. 63*, 207–213.

Bothner-By, A. A., Stephens, R. L., Lee, J., Warren, C. D., & Jeanloz, R. W. (1984) *J. Am. Chem. Soc. 106*, 811–813.

Breslow, E., Beychok, S., Hardman, K. D., & Gurd, F. R. N. (1965) *J. Biol. Chem. 240*, 304–309.

Breslow, E., Chandra, R., & Kappas, A. (1986) *J. Biol. Chem. 261*, 3135–3141.

Brown, S. B., Jones, P., & Lantzke, I. R. (1969) *Nature 223*, 960–961.

Buchler, J. W., Puppe, L., Rohbock, K., & Schneehage, H. H. (1973) *Ann. N.Y. Acad. Sci. 206*, 116–137.

Caughey, W. S. (1980) in *Advances in Inorganic Biochemistry* (Darnall, D. W., & Wilkins, R. G., Eds.) Vol. II, pp 95–115, Elsevier, Amsterdam.

Cocco, M. J., & Lecomte, J. T. J. (1990) *Biochemistry 29*, 11067–11072.

Cooke, R. M., & Wright, P. E. (1987) *Eur. J. Biochem. 166*, 409–414.

Cowan, J. A., & Gray, H. B. (1989) *Inorg. Chem. 28*, 4554–4556.

[5] We have found that minor changes occur in the 450–650-nm region of the optical spectrum, when the reconstitution is performed with SnPP, during the time frame that SnPP·EqMb′ disappears from Figure 6 (Deeb and Peyton, unpublished). A similar result has been found for FePPIX (Gebe et al., 1989).

Deeb, R. S., & Peyton, D. H. (1991) *J. Biol. Chem. 266*, 3728–3733.

Dickerson, R. E., & Geiss, I (1983) *Hemoglobins: Structure, Function, Evolution, Pathology*, Benjamin-Cummings, Menlo Park, CA.

DiFeo, T. J., & Addison, A. W. (1991) *Inorg. Chem. 30*, 1151–1153.

Drummond, G. S., & Kappas, A. (1981) *Proc. Natl. Acad. Sci. U.S.A. 78*, 6466–6470.

Drummond, G. S., & Kappas, A. (1982) *Science 217*, 1250–1252.

Evans, S. V., & Brayer, G. D. (1988) *J. Biol. Chem. 263*, 4263–4268.

Gebe, J. A., Peyton, D. H., & Peyton, J. A. (1989) *Biochem. Biophys. Res. Commun. 161*, 290–294.

Harris, R. K. (1986) *Nuclear Magnetic Resonance Spectroscopy*, Wiley, New York.

Harris, R. K., Kennedy, J. D., & McFarlane, W. (1978) *NMR and the Periodic Table*, pp 342–366, Academic Press, London.

Harrison, S. C., & Blout, E. R. (1965) *J. Biol. Chem. 240*, 299–303.

Hauksson, J. B., La Mar, G. N., Pandey, R. K., Rezzano, I. N., & Smith, K. M. (1990) *J. Am. Chem. Soc. 112*, 6198–6205.

Hoffman, A. B., Collins, D. M., Day, V. W., Fleischer, E. B., Srivastava, T. S., & Hoard, J. L. (1972) *J. Am. Chem. Soc. 94*, 3620–3626.

Hughson, F. M., Wright, P. E., & Baldwin, R. L. (1990) *Science 249*, 1544–1548.

Hunter, C. A., & Sanders, J. K. M. (1990) *J. Am. Chem. Soc. 112*, 5525–5534.

Johnson, C. E., & Bovey, F. A. (1958) *J. Chem. Phys. 29*, 1012–1014.

Jue, T., Krishnamoorthi, R., & La Mar, G. N. (1983) *J. Am. Chem. Soc. 105*, 5701–5703.

Kawamura-Konishi, Y., Kihara, H., & Suzuki, H. (1988) *Eur. J. Biochem. 170*, 589–595.

Kuriyan, J., Wilz, S., Karplus, M., & Petsko, G. A. (1986) *J. Mol. Biol. 192*, 133–154.

La Mar, G. N., Eaton, G. R., Holm, R. H., & Walker, F. A. (1973) *J. Am. Chem. Soc. 95*, 63–75.

La Mar, G. N., Toi, H., & Krishnamoorthi, R. (1984) *J. Am. Chem. Soc. 106*, 6395–6401.

La Mar, G. N., Pande, U., Hauksson, J. B., Pandey, R. K., & Smith, K. M. (1989) *J. Am. Chem. Soc. 111*, 485–491.

La Mar, G. N., Hauksson, J. B., Dugad, L. B., Liddell, P. A., Venkataramana, N., & Smith, K. M. (1991) *J. Am. Chem. Soc. 113*, 1544–1550.

Lecomte, J. T. J., & Cocco, M. J. (1990) *Biochemistry 29*, 11057–11067.

Marion, D., & Wüthrich, K. (1983) *Biochem. Biophys. Res. Commun. 113*, 967–974.

Muller-Eberhard, U. (1988) *Methods Enzymol. 163*, 536–565.

Pasternack, R. F., Francesconi, L., Raff, D., & Spiro, E. (1973) *Inorg. Chem. 12*, 2606–2611.

Sandström, J. (1982) *Dynamic NMR Spectroscopy*, Academic Press, New York.

Scheer, H., & Katz, J. J. (1975) in *Porphyrins and Metalloporphyrins* (Smith, K. M., Ed.) pp 399–524, Elsevier, Amsterdam.

Stong, J. D., & Hartzell, C. R. (1976) *Bioinorg. Chem. 5*, 219–233.

Teale, F. W. J. (1959) *Biochim. Biophys. Acta 35*, 543.

Yee, S., & Peyton, D. H. (1991) *FEBS Lett. 290*, 119–122.